

Synthesis of a Biological-Based Glycoluril with Phosphorous Acid Tags as a New Nanostructured Catalyst: Application for the Synthesis of Novel Natural Henna-Based Compounds

Saeid Moradi,^[a] Mohammad A. Zolfigol,^{*,[a]} Mahmoud Zarei,^{*,[a]} Diego A. Alonso,^{*,[b]} Abbas Khoshnood^{*,[b]}

Abstract:

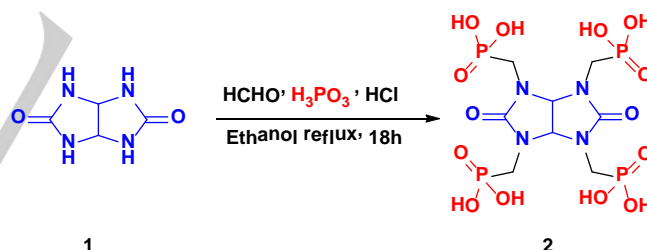
A convenient multicomponent reaction towards the synthesis of natural henna-based 3-methyl-1,4-diphenyl-1,4-dihydrobenzo[6,7]chromeno[2,3-c]pyrazole-5,10-dione derivatives by using a crabby nano glycoluril tetrakis(methylene phosphorous acid) (GTMPA), as an efficient and recyclable catalyst, under neat conditions is described. The major advantages of the synthetic methodology herein described are high yields, short reaction times, and the reusability of the catalyst, which has been fully characterized by Fourier Transform Infrared Spectroscopy (FT-IR), Solid Phosphorus Nuclear Magnetic Resonance (³¹P NMR), Mass spectra (MS), X-Ray Diffraction (XRD), High Resolution Transmission Electron Microscopy (HRTEM), Scanning Electron Microscope (SEM-Mapp.), Energy Dispersive X-Ray (EDX), Thermo Gravimetric Analysis (TGA), Differential Thermal Analysis (DTG), Differential Thermal Analysis (DTA) and X-Ray Photoelectron Spectroscopy (XPS). The described biological-based glycoluril with phosphorous acid pending may be applicable for the synthesis of gels, gelators, self-healing and smart hydrogels.

Introduction

In recent years, there is a great interest in the design and synthesis of easy and safe chemicals and chemical processes.^[1-2] Especially the design of new catalysts and catalytic systems from the viewpoint of green chemistry disciplines are more demand.^[3-6] Among of catalysts, heterogeneous solid catalysts are promising materials widely used when trying to develop simple catalytic and eco-friendly processes due to their easy recyclability by a simple filtration and/or centrifugation, and the potential for reusing as the most important issues.^[7-8] In recent years, researchers are interested in nano-catalysts because of their high specific surface area and hence the high activity and selectivity usually shown by these materials.^[9-14] On the other hand, multicomponent reactions (MCRs) have become a very important tool in organic chemistry because three or more starting materials react to form a product, which all or most of the atoms contribute to the final product.^[15-17] This type of

reactions have been widely used in the synthesis of complex pharmaceutically active heterocyclic compounds,^[18-20] especially nitrogen-containing derivatives due to the biological activity usually shown by this type of compounds.^[21-23] Functionalized quinone- and naphthoquinone derivatives are molecules often obtained from natural sources (henna's leaves, *Streptococcus dunnii*,...) which have been widely used as synthetic intermediates in both academia and industry due to their interesting biological and drug-like properties.^[24-35] On the other hand, glycoluril as a biological urea based precursor has been used for various purposes.^[36]

In this paper the synthesis and characterization of a new glycoluril tetrakis(methylene phosphorous acid) (GTMPA)-derived solid acid nano-catalyst **2** is reported (Scheme 1). Also, we present an efficient and green **2**-catalyzed MCR towards the synthesis of 3-methyl-1,4-diphenyl-1,4-dihydrobenzo[6,7]chromeno[2,3-c]pyrazole-5,10-dione derivatives.



Scheme 1. Synthesis of nanostructured catalyst **2**.

[a] S. Moradi, Prof. M. A. Zolfigol, Dr. M. Zarei
Department of Organic Chemistry, Faculty of Chemistry, Bu-Ali Sina University, Hamedan 6517838683, Tel: +988138282807, Fax: +988138380709 Iran. E-Mail: zolfi@basu.ac.ir & mzolfigol@yahoo.com (Mohammad Ali Zolfigol) or Mahmoud Zarei (mahmoud8103@yahoo.com).

[b] Dr. D. A. Alonso, Dr. A. Khoshnood
Organic Synthesis Institute, and Organic Chemistry Department, Alicante University, Apdo. 99, 03080 Alicante, Spain. E-Mail: diego.alonso@ua.es (Diego A. Alonso) and abbas.khoshnood@ua.es (Abbas Khoshnood)

Supporting information for this article is given via a link at the end of the document.

Results and Discussion

Initially, we synthesized the heterogeneous nano-catalyst **2** by a one-step *N*-peralkylation of glycoluril (**1**) with paraformaldehyde and phosphorous acid in refluxing EtOH (Scheme 1). This material was characterized using different techniques such as, FT-IR, ^{31}P NMR, Mass spectra, X-ray diffraction patterns (XRD), scanning electron microscopy (SEM) with elemental mapping and EDX, high resolution transmission electron microscopy (HRTEM), thermogravimetry (TG), derivative thermogravimetry (DTG) analysis, differential thermal

analysis (DTA), and X-ray photoelectronic spectroscopy (XPS) (Figure 1-8).

As shown in Fig. 1 the FT-IR spectrum of **2** showed an absorption band at 3200 cm^{-1} corresponding to the OH stretching frequency of the phosphorous acid. Furthermore, the absorption band at 1678 cm^{-1} certified the presence of the amide carbonyl moiety and peaks related to P=O, C-P and C-N bond were observed at 1219, 1110 and 991 cm^{-1} respectively (Figure 1).

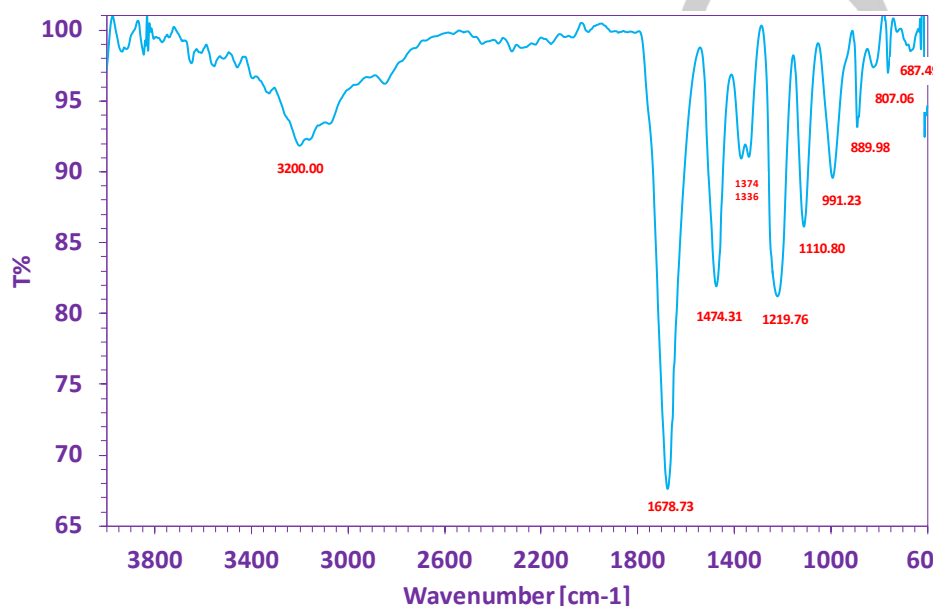


Fig. 1. FT-IR spectrum of GTMPA

On the other hand, the solid ^{31}P NMR spectrum of **2** showed the signal of the hydrogen-bonded P-OH protons as a single resonance at 10.74 ppm, confirming the presence of the phosphorous acid moiety in the catalyst (Figure 2), white solid, M. P: $>300\text{ }^{\circ}\text{C}$ and Mass spectra of **2** showed MS m/z (%): 519 (M^+ , 1) (Figure 3).

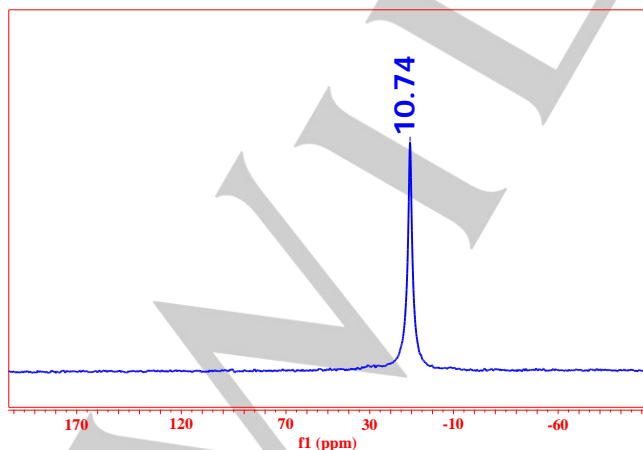


Fig. 2. ^{31}P NMR spectrum (solid state, 202 MHz) of catalyst **2**.

The X-ray diffraction (XRD) pattern of the catalyst was considered in a domain of 5 to 70 degree. Peak width (FWHM), size and inter planer distance related to XRD pattern of **2** were

investigated in the 17.1 to 38.3 degree (Fig. 4). The obtained data is collected in Table 1. The crystallite size D of the solid catalyst was calculated using the Debye–Scherrer formula $D = K\lambda/(\beta\cos\theta)$, with λ being the X-ray wavelength ($\lambda = 0.154\text{ nm}$), K is the Scherrer constant (0.9), β the peak width of half-maximum (FWHM), and θ is the Bragg diffraction angle. The interplanar distance was calculated via the Bragg equation: $d_{hkl} = \lambda/(2\sin\theta)$, (λ : Cu radiation (0.154178 nm). Finally, the crystal dimensions from various diffraction lines using the Scherrer equation were found to be in the nanometer range (29.06 - 47.31 nm).

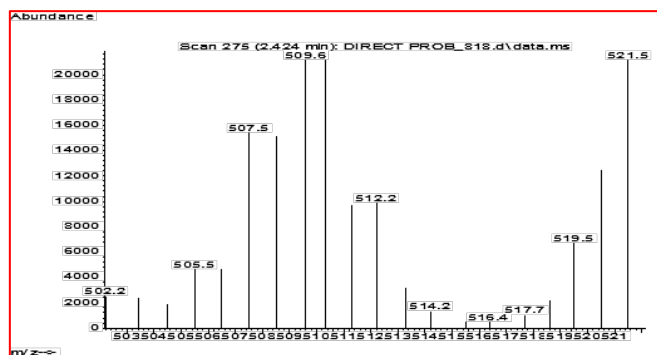


Fig. 3. Mass spectra of GTMPA

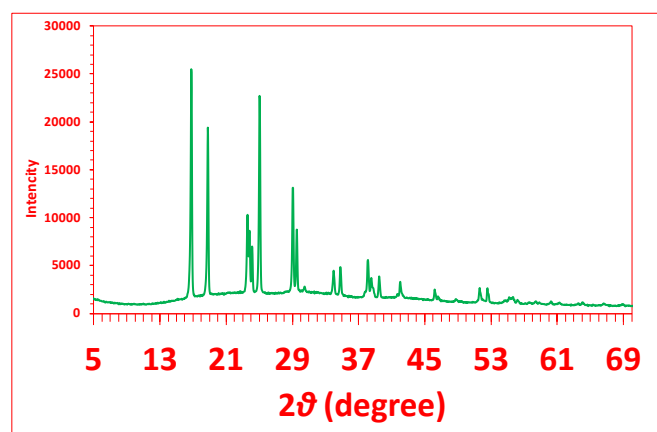


Fig. 4. XRD pattern of 2.

Table 1. X-ray diffraction (XRD) data of GTMPA.

Entry	2θ	Peak width (degree) (FWHM)	Size [nm]	Inter planar distance [nm]
1	17.1	0.2	40.16	0.51851
2	19.1	0.3	26.87	0.46465
3	23.9	0.3	27.09	0.37231
4	25.3	0.3	27.16	0.35201
5	29.3	0.3	27.39	0.30480
6	35	0.3	27.79	0.25636
7	38.3	0.5	16.82	0.23410

The surface typical textural and morphological properties of the catalyst and the difference in adhesion and dispersion can be clearly studied from the HRTEM, SAED, SEM and elemental SEM-mapping images as exposed in Fig. 5a-h. Initially, we used high-resolution transmission electron microscopy (HRTEM) to study the detailed structure of the solid catalyst **2**. Figures 5a and b show the HRTEM image of **2** supported on a TEM copper grid. Also, the combined selected area electron diffraction (SAED) patterns of the catalyst are shown in Figure 5c. The HRTEM images of the catalyst showed near spherical nanoparticles morphology with an appropriate mono disparity. Moreover, we also analyzed the morphology of catalyst **2** using scanning electron microscopy (SEM). As depicted in Figure 5d for the SEM micrograph, and Figures 5e-h for the SEM-elemental mapping (C, N, O and P), the presence of C, N, O and P elements in the catalyst with a good distribution over the catalyst surface was verified.

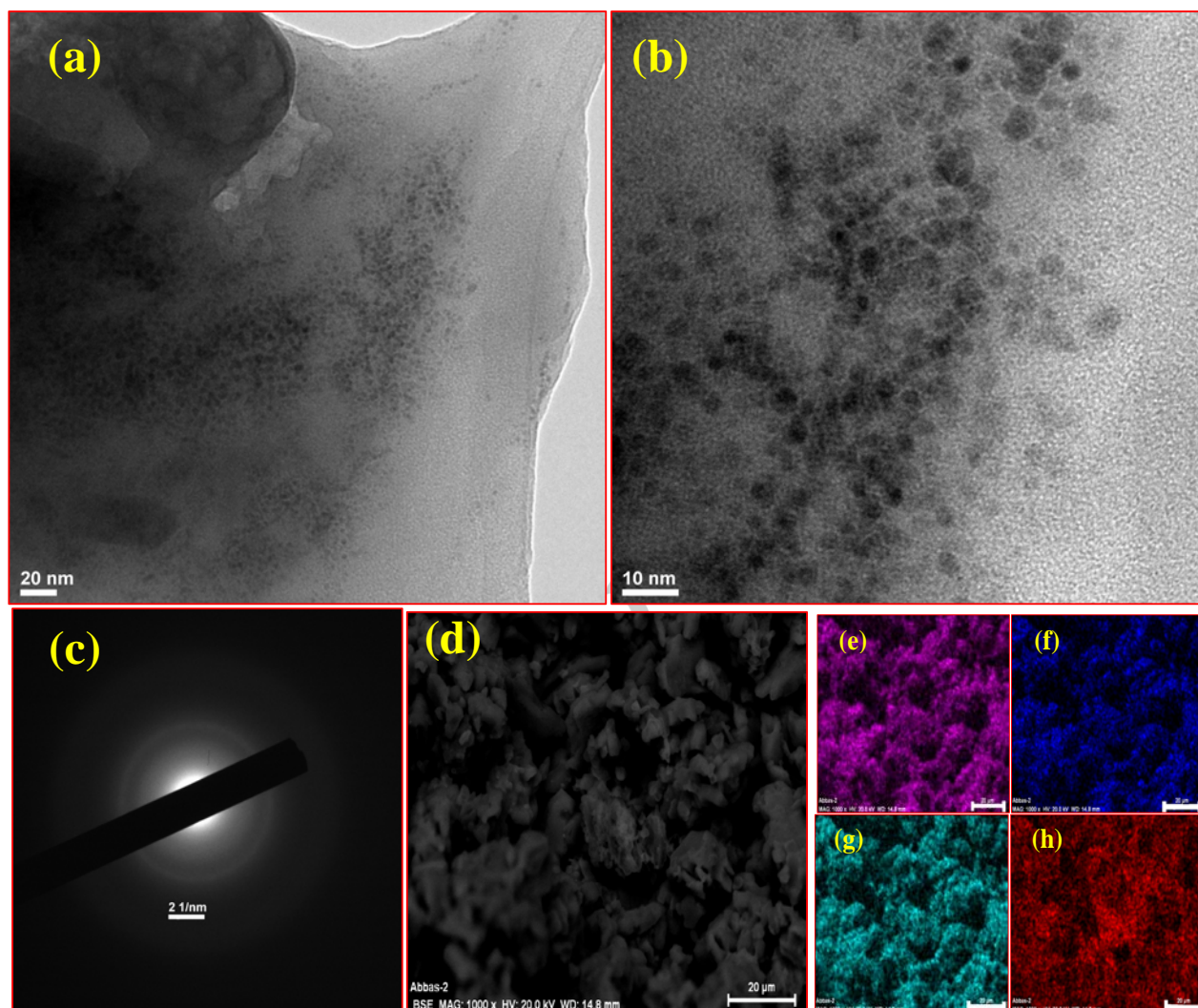


Fig. 5. High resolution transmission electron microscopy (HRTEM) (a-b), selected area electron diffraction (SAED) (c), scanning electron microscopy (SEM) of glycoluril (d); elemental maps (EDX) of N (e); C (f); P (g) and O (h) atoms for catalyst 2.

Fig. 6 collects representative energy-dispersive X-ray spectroscopy (EDS) elemental distribution images of catalyst 2, which corroborated the existence of phosphorus on the catalyst structure in a ~2 wt %. The elemental analysis also showed a 43 wt% of carbon, a 29 wt% of nitrogen and a 26 wt% of oxygen.

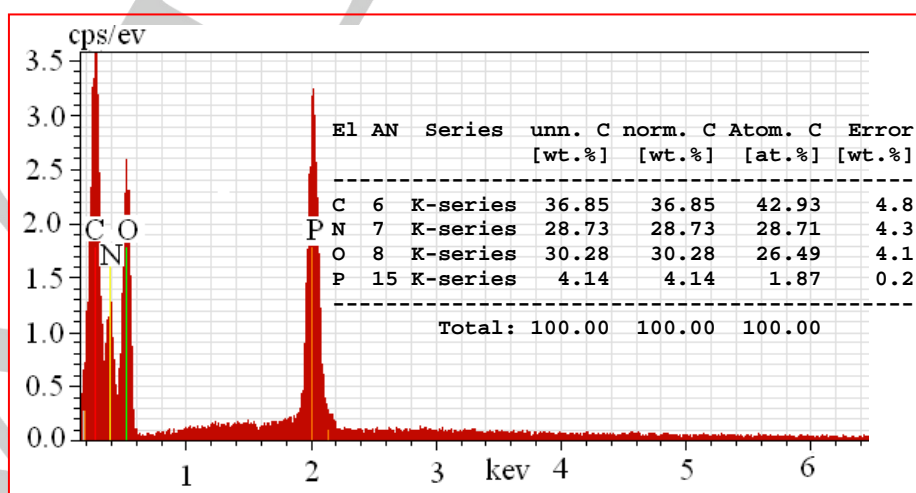


Fig. 6. Energy-Dispersive X-ray spectroscopy (EDS) analysis of **2**.

In order to monitor the thermal stability and behavior of the GTMPA-derived catalyst, the thermogravimetric analysis (TGA), derivative thermogravimetric analysis (DTG), as well as the differential thermal analysis (DTA) were conducted (Fig. 7 a and b). Regarding TGA, a first weight loss stage, related to the removal of surface-adsorbed water and organic solvents, took place between 25 and 100 °C, involving a weight loss of 2.2%.

The main weight loss, associated with the decomposition of the catalyst, took place around 200-400 °C in a single exothermic step manner and involved a weight loss of 39.5%. Moreover, the DTA analysis diagram showed a general negative downward slope between 25 °C to 700 °C in which, decomposition of catalyst and its precursor in nitrogen atmosphere were exothermic (Fig. 7b).

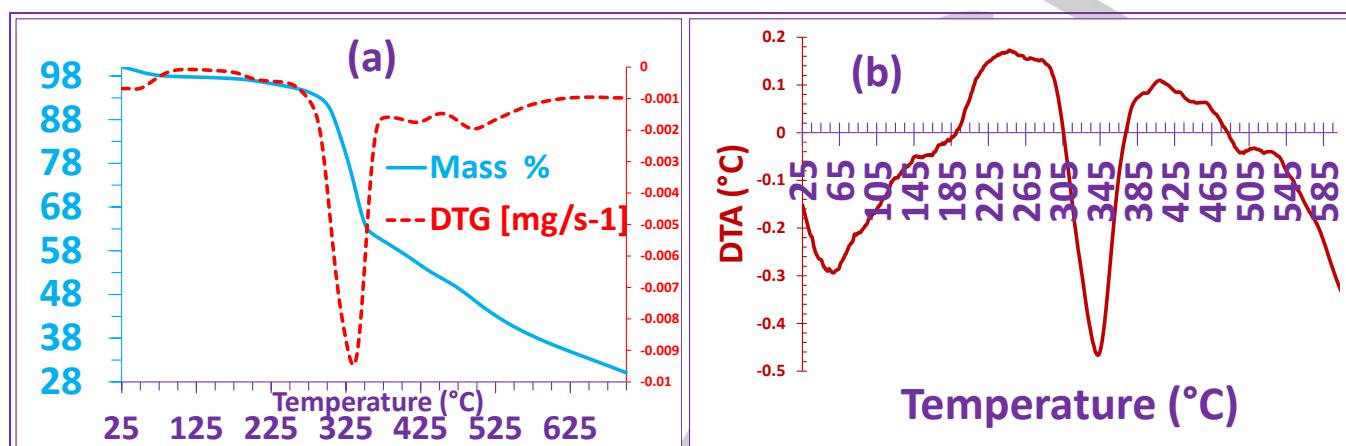


Fig. 7. Thermal stability and behavior of **2**: (a) thermogravimetric analysis (TGA) and derivative thermogravimetric analysis (DTG); (b) differential thermal analysis (DTA).

Additional studies with X-ray photoelectron spectra (XPS) were carried out to analyze the surface character and chemical composition of the prepared catalyst **2**. As expected, the peaks corresponding to N1s, O1s, C1s, and P2p were clearly seen in the XPS survey spectrum of catalyst **2**, thus confirming the presence of the phosphonomethyl ($-\text{CH}_2\text{PO}_3\text{H}_2$) moiety covalently bonded to **1** (Figure 8a). As shown in Figure 8b, the phosphorus peaks located around 133.68 eV could be fitted into two 2p peaks located at 133.45 (C-P-O) and 134.35 (C-P=O) eV corresponding to 2p_{3/2} and 2p_{1/2} level, respectively in an area ratio 1/0.5. Moreover, the C1s XPS spectrum of glycoluril could be deconvoluted into three peaks at 284.62, 287.08, 288.73 eV fitted with a broad peak at 285.70 eV. These energies confirmed the existence of CH-CH, N-CH₂-P, N-C=O and N-CH=N moieties, respectively in an area ratio of 0.7/1/1/0.2 and an atomic

percentage of 11.7/15.9/15.8/3.2. From the same atomic percentage and area ratio showed by the groups C=O and C-P, we could reason that the surface of catalysts was principally covered by these two carbon moieties. On the other hand, the symmetrical N1s XPS spectrum of **2**, located around 399.68 eV, could be deconvoluted into one peak at 399.66 eV which revealed the existence of N-C=O. This peak should be fitted with a broader peak (higher FWHM) with a 0.01 eV binding energy difference at 400.66 eV in an area ratio of 1/0.1.^[37] This second broad peak suggests the presence of secondary amides in the catalyst. Finally, the unsymmetrical oxygen peaks located around 531.48 eV could be fitted into two 1s peaks located at 531.37 (C-P=O) and 532.71 (N-C=O) eV in an area ratio of 1/0.8.^[38]

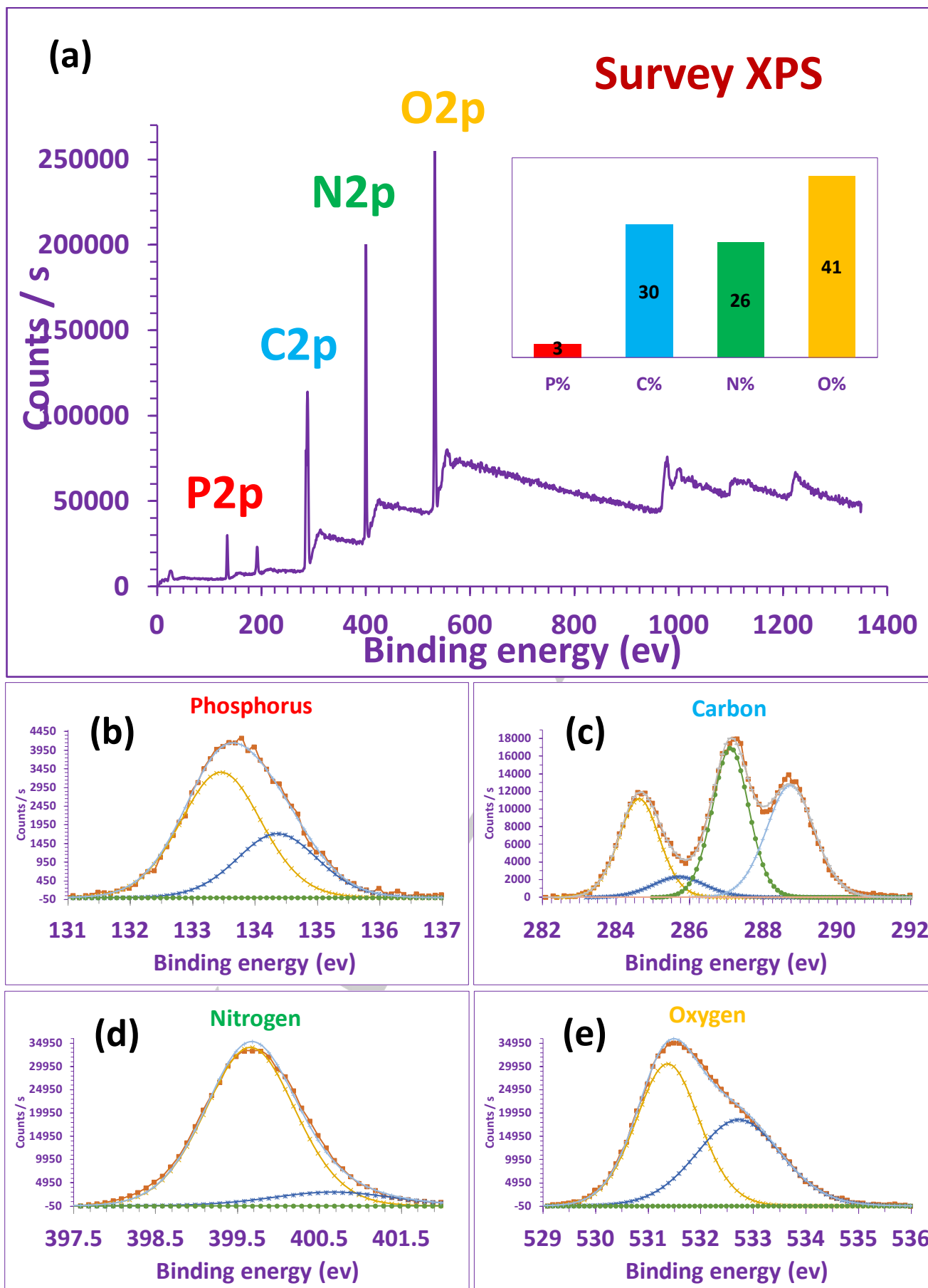
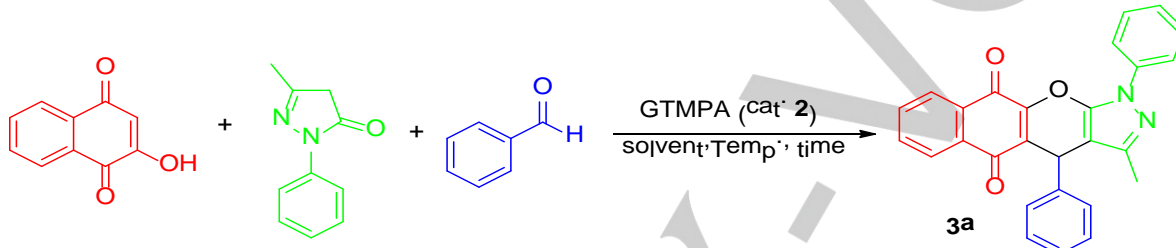


Fig. 8. X-ray photoelectron spectra (XPS) survey spectrum (a); and high resolution XPS spectra of P2p (b); C1s (c); N1s (d); and O1s (e) of GTMPA

After characterization of catalyst **2**, we studied its catalytic activity as solid acid in the multicomponent synthesis of 3-methyl-1,4-diphenyl-1,4-dihydrobenzo[6,7]chromeno[2,3-c]pyrazole-5,10-dione derivatives. In order to optimize the reaction conditions, the condensation reaction of benzaldehyde, 2-hydroxynaphthalene-1,4-dione and 3-methyl-1-phenyl-1*H*-pyrazol-5(4*H*)-one to obtain compound **3a** was chosen as a model reaction. Initially, optimization of the catalyst loading and reaction temperature was carried out under neat conditions (Table 2). As shown, low yields were obtained in the absence of catalyst both at 25 and 100 °C

(Table 2, entries 1 and 2). At 100 °C, the optimal catalyst loading was 5 mol% (Table 2, entries 3-6). Regarding temperature, the process was still highly efficient even working at 50 °C using 5 mol% of **2** (Table 2, entry 8). Regarding solvent optimization, the model reaction (Scheme 1) was carried out using various solvents (EtOAc, CH₃CN, EtOH and H₂O) in the presence of **2** (5 mol%) under reflux conditions. As summarized in Table 2 (entries 9-12), no solvent afforded better yield than using neat conditions even running the reaction for 2 h (entry 8).

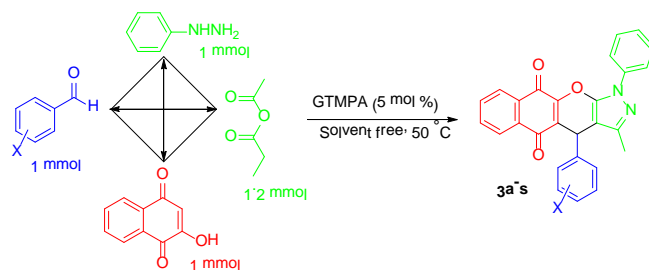
Table 2. Synthesis of **3a** under neat conditions. Catalyst loading, temperature and solvent optimization.



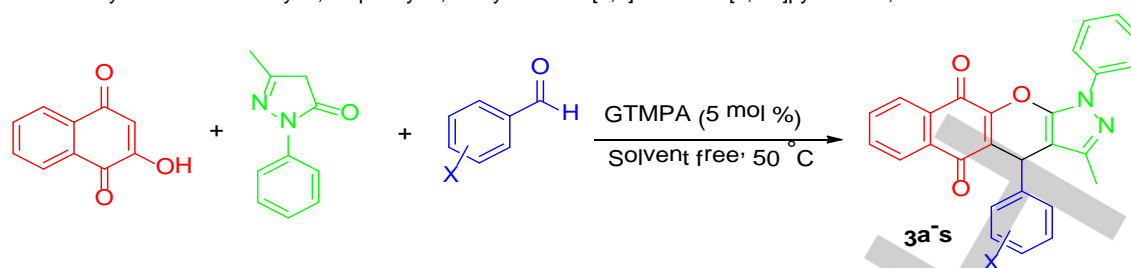
Entry	Solvent	Cat 2 (mol%)	Temp (°C)	Time (min)	Isolated Yield (%)
1	-	-	25	50	55
2	-	-	110	50	10
3	-	2	100	15	75
4	-	5	100	15	94
5	-	10	100	15	70
6	-	15	100	15	65
7	-	5	75	15	92
8	-	5	50	15	91
9	EtOAc	5	Reflux	120	< 5
10	MeCN	5	Reflux	120	63
11	EtOH	5	Reflux	120	35
12	H ₂ O	5	Reflux	120	75

After optimization of the reaction conditions, the efficiency and applicability of the method were studied by reaction of 2-hydroxynaphthalene-1,4-dione and 3-methyl-1-phenyl-1*H*-pyrazol-5(4*H*)-one with various aromatic aldehydes in the presence of GTMPA (5 mol%) under neat conditions. Table 3 summarizes the results which demonstrates the wide scope of the methodology since all the tested functionalized aldehydes (neutral, electron-rich and electron-poor) afforded the desired 3-methyl-1,4-diphenyl-1,4-dihydrobenzo[6,7]chromeno[2,3-c]pyrazole-5,10-dione derivatives in high to excellent yields (86-95%) in very short reaction times (5-14 min). Interestingly, the tetra component version of the reaction (see experimental section, Method B), with the in situ generation of 3-methyl-1-phenyl-1*H*-pyrazol-5(4*H*)-one from phenylhydrazine and ethyl acetoacetate, was also efficient towards the synthesis of the

target products, as demonstrated with the synthesis of products (Scheme 2).



Scheme 2. Synthesis of 3-methyl-1,4-diphenyl-1,4-dihydrobenzo[6,7]chromeno[2,3-c]pyrazole-5,10-dione using **2**.

Table 3. Synthesis of 3-methyl-1,4-diphenyl-1,4-dihydrobenzo[6,7]chromeno[2,3-c]pyrazole-5,10-dione derivatives.

Entry	Aldehyde		Time (min) A/B	Yield (%) A/B	M.P. (°C)
1	Benzaldehyde	3a	7/9	91/88	146-148
2	4-Chlorobenzaldehyde	3b	5/6	95/92	148-150
3	2-Chlorobenzaldehyde	3c	6/7	92/90	247-249
4	3-Nitrobenzaldehyde	3d	6/9	93/91	245-247
5	4-Methylbenzaldehyde	3e	9/13	89/86	239-241
6	2-Hydroxybenzaldehyde	3f	11/13	88/86	207-209
7	3-Hydroxybenzaldehyde	3g	9/12	89/85	240-242
8	4-Nitrobenzaldehyde	3h	5/6	96/95	235-237
9	2,4-Dichlorobenzaldehyde	3i	5/7	92/90	247-249
10	4-Fluorobenzaldehyde	3j	6/8	93/91	238-240
11	4-Methoxybenzaldehyde	3k	11/14	89/87	228-230
12	2-Hydroxy-1-naphthaldehyde	3l	13/17	88/84	247-249
13	Terephthalaldehyde	3m	10/15	92/89	210-212
14	2,6-Difluorobenzaldehyde	3n	7/9	90/92	247-249
15	4-(Trifluoromethyl) benzaldehyde	3o	10/12	90/91	210-212
16	4-Formylbenzonitrile	3p	11/13	92/90	228-230
17	3,5-Difluorobenzaldehyde	3q	10/11	90/89	226-228
18	Thiophene-2-carbaldehyde	3r	15/19	82/77	230-232
19	Furan-2-carbaldehyde	3s	18/23	81/76	210-213

A catalytic cycle proposal for the multicomponent synthesis of 3-methyl-1,4-diphenyl-1,4-dihydrobenzo[6,7]chromeno[2,3-c]pyrazole-5,10-dione derivatives is shown in Scheme 3. As shown, the aldehyde is initially activated by GTMPA towards the nucleophilic attack of 2-hydroxynaphthalene-1,4-dione affording, after dehydration, the 3-methylenenaphthalene intermediate **I**. Then, 5-methyl-2-phenylpyrazolidin-3-one (obtained from ethyl acetoacetate and phenyl hydrazine following Method B) reacts via conjugate addition with **I** to afford adduct **II**, which suffers an intramolecular cyclization/dehydration process assisted by **2** to give intermediate **III**. A final 2-assisted deprotonation of **III** yields the reaction product.

The recyclability and reuse of the catalyst was also studied on the reaction of benzaldehyde (1mmol), 2-hydroxynaphthalene-1,4-dione (1mmol) and 3-methyl-1-phenyl-1*H*-pyrazol-5(4*H*)-one (1mmol) at 50 °C. After completion the

reaction as monitored by TLC, EtOAc (10 mL) was added to the reaction mixture, the catalyst was separated from solution using a centrifugation (1000 rpm). The remained catalyst was washed with hot acetone (10 mL), dried and was used for the next runs. As indicated in Fig. 9, catalyst could be recycled and efficiently reused up to 8 reaction cycles with no detectable loss of catalytic activity.

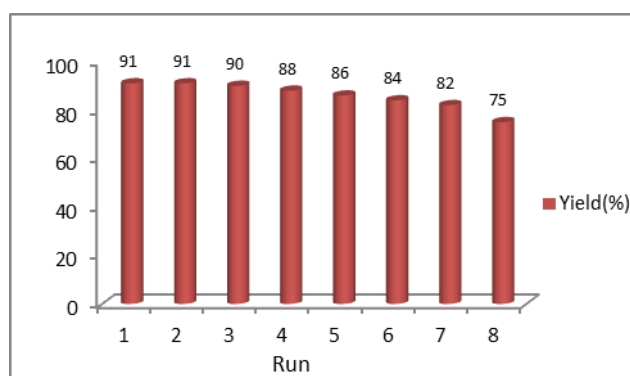
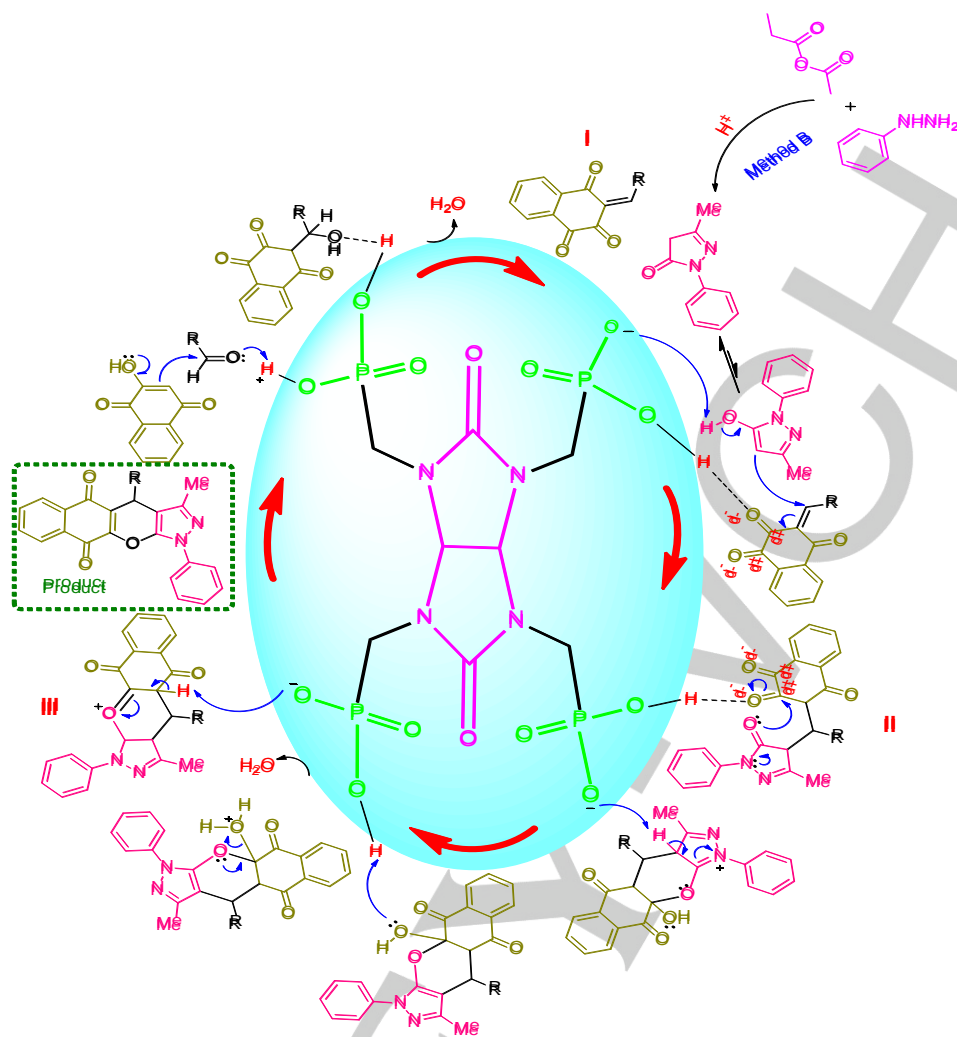


Fig. 9. Recyclability of **2** as catalyst in the synthesis of 3-methyl-1,4-diphenyl-1,4-dihydrobenzo[6,7]chromeno[2,3-c]pyrazole-5,10-dione under solvent free condition at 50 °C. Reaction time 8 min.



Scheme 3. Mechanism for the 2-catalyzed synthesis of 3-methyl-1,4-diphenyl-1,4-dihydrobenzo[6,7]chromeno[2,3-c]pyrazole-5,10-diones under solvent free conditions

Conclusions

In conclusion, herein we present the preparation of a crabby biological-based glycoluril tetrakis(methylene phosphorous acid) (GTMPA) for the first time. Two convenient methods for the synthesis of novel biological henna-based 3-methyl-1,4-diphenyl-1,4-dihydrobenzo[6,7]chromeno[2,3-c]pyrazole-5,10-diones were also reported in the presence of described nano glycoluril tetrakis(methylene phosphorous acid) (GTMPA) as an efficient and recyclable catalyst under neat conditions. The major advantages of the presented method are high yields, short reaction times, and the reusability of the catalyst. We think that the present work can open up a new and promising insight in the course of rational design, synthesis and application of other biological-based, task-specific and advanced

nano materials with phosphorous acid tags for various purposes. The described biological-based glycoluril with phosphorous acid pending may be useful for the synthesis of gels, gelators, self-healing and smart hydrogels. Further systematic research for knowledge-based development of this research field is going on in our research group.

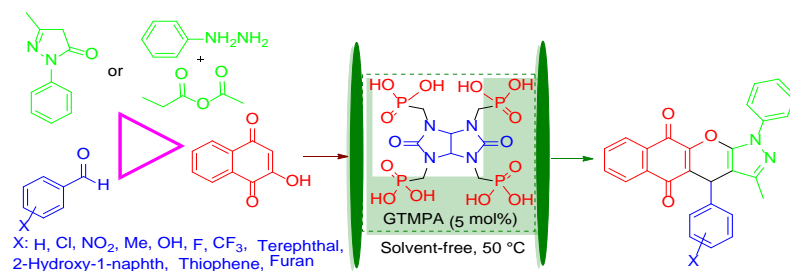
Acknowledgements

We thank Bu-Ali Sina University, Iran National Science Foundation (INSF) (Grant Number: 96003376), National Elites Foundation, University of Alicante (VIGROB-173, UAU116-03), and the Spanish Ministerio de Economía y Competitividad (CTQ2015-66624-P) for financial support to our research groups.

Keywords: Glycoluril, Glycoluril tetrakis(methylene phosphorous acid) (GTMPA), Biological-based, Nanostructured catalyst,

Recyclable catalyst, 3-Methyl-1,4-diphenyl-1,4-dihydrobenzo[6,7]chromeno[2,3-c]pyrazole-5,10-dione.

- [1] P. T. Anastas, J. B. Zimmerman, *Green Chem.* **2016**, *18*, 4324-4324.
- [2] P. T. Anastas, J. C. Warner, *Green Chemistry: Theory and Practice*, Oxford University Press: New York, **1998**.
- [3] G. Mohammadi Ziarani, N. Lashgari, A. Badiiei, *J. Mol. Catal. A: Chem.* **2015**, *397*, 166-191.
- [4] M. Kaur, S. Sharma, P. M. S. Bedi, *Chin. J. Catal.* **2015**, *36*, 520-549.
- [5] F. Su, Y. Guo, *Green Chem.* **2014**, *16*, 2943-2957.
- [6] Y. M. Sani, W. M. A. W. Daud, A. R. Abdul Aziz, *Appl. Catal. A: Gen.* **2014**, *470*, 140-161.
- [7] R. M. N. Kalla, H. Park, T. T. K. Hoang, I. Kim, *Tetrahedron Lett.* **2014**, *55*, 5373-5376.
- [8] W. Xie, H. Wang, H. Li, *Ind. Eng. Chem. Res.* **2012**, *51*, 225-231.
- [9] M. A. Zolfigol, V. Khakyzadeh, A. R. Moosavi-Zare, A. Rostami, A. Zare, N. Iranpoor, M. H. Beyzavi, R. Luque, *Green Chem.* **2013**, *15*, 2132-2140.
- [10] M. Daraei, M. A. Zolfigol, F. Derakhshan-Panah, M. Shiri, H. G. Kruger, M. Mokhleshi, *J. Iran. Chem. Soc.* **2015**, *12*, 855-861.
- [11] M. Mokhtary, *J. Iran. Chem. Soc.* **2016**, *13*, 1827-1845.
- [12] M. A. Zolfigol, H. Ghaderi, S. Bagheri, L. Mohammadi, *J. Iran. Chem. Soc.* **2017**, *14*, 121-134.
- [13] V. Polshettiwar, R. S. Varma, *Green Chem.* **2010**, *12*, 743-754.
- [14] F. Cao, P. Yin, X. Liu, C. Liu, R. Qu, *Renew. Energy* **2014**, *71*, 61-68.
- [15] R. V. A. Orru, M. D. Greef, *Synthesis* **2003**, *10*, 1471-1499.
- [16] V. Nair, C. Rajesh, A. U. Vinod, S. Bindu, A. R. Sreekanth, J. S. Mathen, L. Balgopal, *Acc. Chem. Res.* **2003**, *36*, 899-907.
- [17] L. F. Tietze, A. Modi, *Med. Chem. Res.* **2000**, *20*, 304-322.
- [18] E. Abbaspour-Gilandeh, M. Aghaei-Hashjin, P. Jahanshahi, M. S. Hoseininezhad-Namin, *Monatsh Chem.* **2017**, *148*, 731-738.
- [19] F. Al-Assar, K. N. Zelenin, E. E. Lesiovskaya, I. P. Bezhan, B. A. Chakchir, *Pharm. Chem.* **2002**, *36*, 598-603.
- [20] R. P. Jain, J. C. Vederas, *Bioorg. Med. Chem. Lett.* **2004**, *14*, 3655-3658.
- [21] S. Kumar, H. Ila, H. Junjappa, *J. Org. Chem.* **2009**, *74*, 7046-7051.
- [22] M. Li, Y.-L. Hou, L.-R. Wen, F.-M. Gong, *J. Org. Chem.* **2010**, *75*, 8522-8532.
- [23] S. Rostamnia, A. Hassankhani, *RSC Adv.* **2013**, *3*, 18626-18629.
- [24] R. H. Thomson, *Naturally occurring quinones*. 4th ed. London, Chapman & Hall, **1997**.
- [25] S. Subramanian, M. M. C. Ferreira, M. Trsic, *J. Struct. Chem.* **1998**, *9*, 47-57.
- [26] A. F. Santos, P. A. L. Ferraz, A. V. Pinto, M. C. F. R. Pinto, M. O. F. Goulart, A. E. G. Sant'Ana, *Int. J. Parasitol.* **2000**, *30*, 1199-1202.
- [27] M. J. Teixeira, Y. M. De Almeida, J. R. Viana, J. G. Holanda Filha, T. P. Rodrigues, J. R. C. Prata Jr, *Phytother. Res.* **2001**, *15*, 44-48.
- [28] E. R. De Almedia, A. A. D. S. Filho, E. R. D. Santos, C. A. C. Lopes, *J. Ethnopharmacol.* **1990**, *29*, 239-241.
- [29] S. Garnier, J. L. Wolfender, M. Nianga, H. Stoeckli-Evans, K. Hostettmann, *Phytochemistry* **1996**, *42*, 1315-1320.
- [30] B. S. Siddiqui, M. N. Kardar, T. Ali, S. Khan, *Helv. Chim. Acta.* **2003**, *86*: 2164-2169.
- [31] A. L. Perez, G. Lamoureux, A. Sanchez-Kopper, *Tetrahedron Lett.* **2007**, *48*, 3735-3738.
- [32] M. Dabiri, Z. Noroozi Tisseh, A. Bazgir, *Dyes and Pigments* **2011**, *89*: 63-69.
- [33] V. K. Tandon, H. K. Maurya, *Tetrahedron Lett.* **2009**, *50*, 5896-5902.
- [34] V. K. Tandon, H. K. Maurya, *Tetrahedron Lett.* **2010**, *51*, 3843-3847.
- [35] H. B. Zhang, L. Liu, Y. J. Chen, D. Wang, C. J. Li, *Eur. J. Org. Chem.* **2006**, 869-873.
- [36] a) A. Yaghoubi, M. G. Dekamin, *Chem. Select.* **2017**, *2*, 9236 - 9243; b) K. I. Assaf, W. M. Nau, *Chem. Soc. Rev.* **2015**, *44*, 394-418; c) J. Mohanty, *Encyclopedia of Polymer Science and Technology*, DOI: 10.1002/0471440264.pst639; d) P. I. Dalko, L. Moisan, *Angew. Chem. Int. Ed.* **2001**, *40*, 3726-3748; e) P. I. Dalko, L. Moisan, *Angew. Chem. Int. Ed.* **2004**, *116*, 5248-5286; f) C. Bolm, *Adv. Synth. Catal.* **2004**, *346*, 1022-1022; g) M. G. Dekamin, S. Ilkhanizadeh, Z. Latifidoost, H. Daemi, Z. Karimi, M. Barikani, *RSC Adv.* **2014**, *4*, 56658-56664.
- [37] L. N. Bui, M. Thompson, N. B. McKeown, A. D. Romaschin and P. G. Kalman, *Analyst* **1993**, *118*, 463-474.
- [38] P. Y. Shih, S. W. Yung, T. S. Chin, *J. non-Crystalline Solids* **1999**, *244*, 211-222.



Saeid Moradi,^a
Mohammad Ali
Zolfigol,^{*,a}
Mahmoud Zarei,^{*,a}
Diego A. Alonso,^{*,b}
Abbas
Khoshnood^{*,b}

Page No. – Page
No.

Title

Additional Author information for the electronic version of the article.

^aDepartment of Organic Chemistry, Faculty of Chemistry, Bu-Ali Sina University, Hamedan 6517838683, Tel: +988138282807, Fax: +988138380709 Iran. E-Mail: zolfi@basu.ac.ir & mzolfigol@yahoo.com (Mohammad Ali Zolfigol), mahmoud8103@yahoo.com (Mahmoud Zarei).

^bOrganic Synthesis Institute and Organic Chemistry Department, Alicante University, Apdo. 99, 03080 Alicante, Spain. E-Mail: diego.alonso@ua.es (Diego A. Alonso), abbas.khoshnood@ua.es (Abbas Khoshnood)

WILEY-VCH